New Phytologist Supporting Information

MoErv29 promotes apoplastic effector secretion contributing to virulence of the rice blast fungus *Magnaporthe oryzae*

Bin Qian, Xiaotong Su, Ziyuan Ye, Xinyu Liu, Muxing Liu, Danyu Shen, Han Chen, Haifeng Zhang, Ping Wang, and Zhengguang Zhang

1 November 2021

Figure S1. Eight sites mutation were introduced to prevent splicing by UPR.

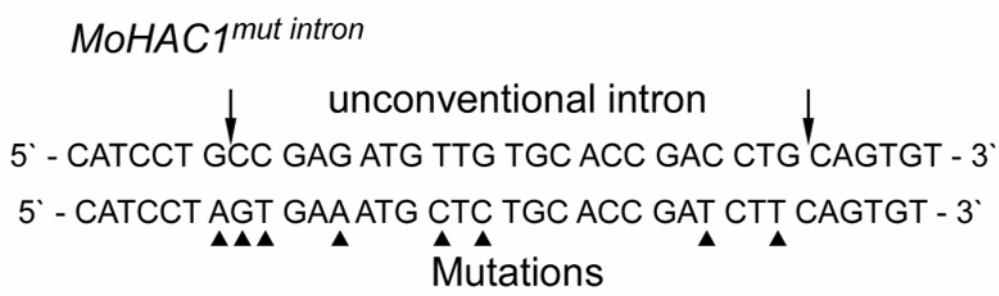

Figure S2. Yeast complementation assay.

MoERV29 could partially suppress the growth defect of the yeast Δ*Scerv29* mutant under 50 μg/ml DTT stress. The yeast Δ*ScERV29* mutant was complemented with *MoERV29* cDNA. Yeast wild-type strain BY4741 and the Δ*Scerv29* mutant transformed with empty pYES2 vector were used as controls. Serial dilutions of cell suspensions of each strain were spotted on SD and SD+DTT plates for four 4 days and photographed.

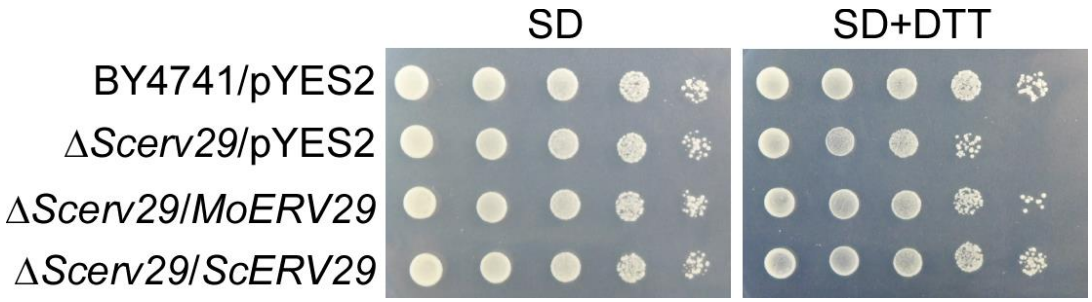

Figure S3. Gene knockout strategy and expression analyses in *M. oryzae.*

(A) The *MoERV29* gene knockout schematics. (B) PCR analysis of the *MoERV29* deletion mutants. (C) Southern blot analysis of the *MoERV29* deletion mutants. The genomic DNA of Guy11 and Δ*MoERV29* mutants were digested with *Sma* I and hybridized with *MoERV29* and *HPH* probe, respectively. (D) qRT-PCR analysis of the expression of *MoERV29* in the indicated strains. Error bars represent ± SD, and asterisks represent significant differences (p<0.01).

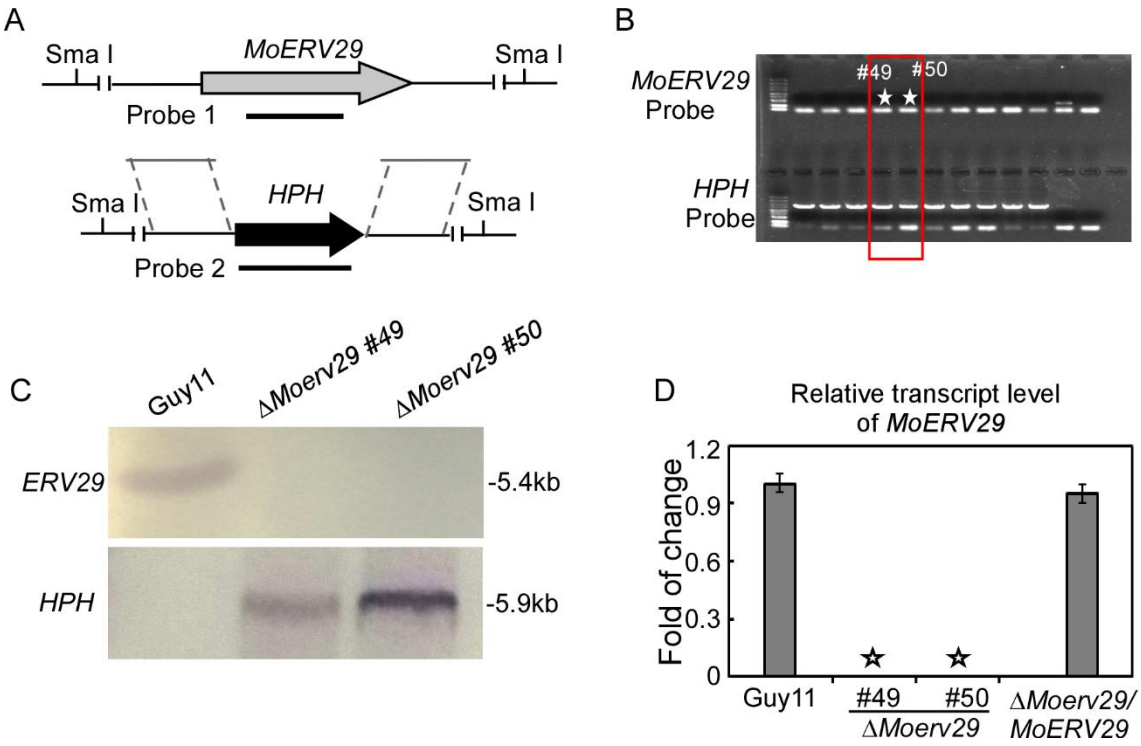

Figure S4. Expression profiles of *MoERV29* during various developmental stages

Expression levels of *MoERV29* during different stages of *M. oryzae*. Expression in the hyphal stage was used as the internal reference. Error bars represent ± SD.

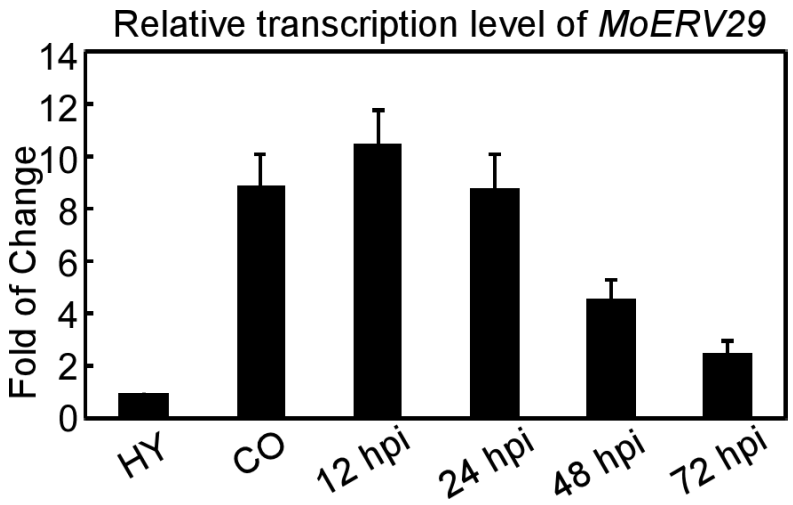

Figure S5. MoErv29 partially co-located with ER and Golgi.

(A) The co-localization patterns of MoErv29-GFP with ER marker MoLhs1-RFP and the Golgi marker MoSft2-RFP, respectively. Insets highlight areas analyzed by line-scan, and the histogram indicates the percentage of MoErv29-GFP in ER and Golgi, NT = Not Treatment. (B) The co-localization observation of MoErv29-GFP with ER and Golgi under BFA treatment. Insets highlight areas analyzed by line-scan, and the histogram indicates the percentage of MoErv29-GFP in ER and Golgi. (C) The co-localization of MoErv29-GFP with ER and Golgi under DMSO control. (Bar = 10 μm). The white stars in merge panels indicate the merged vesicles. Error bars represent ± SD, and asterisks represent significant differences (p<0.01)

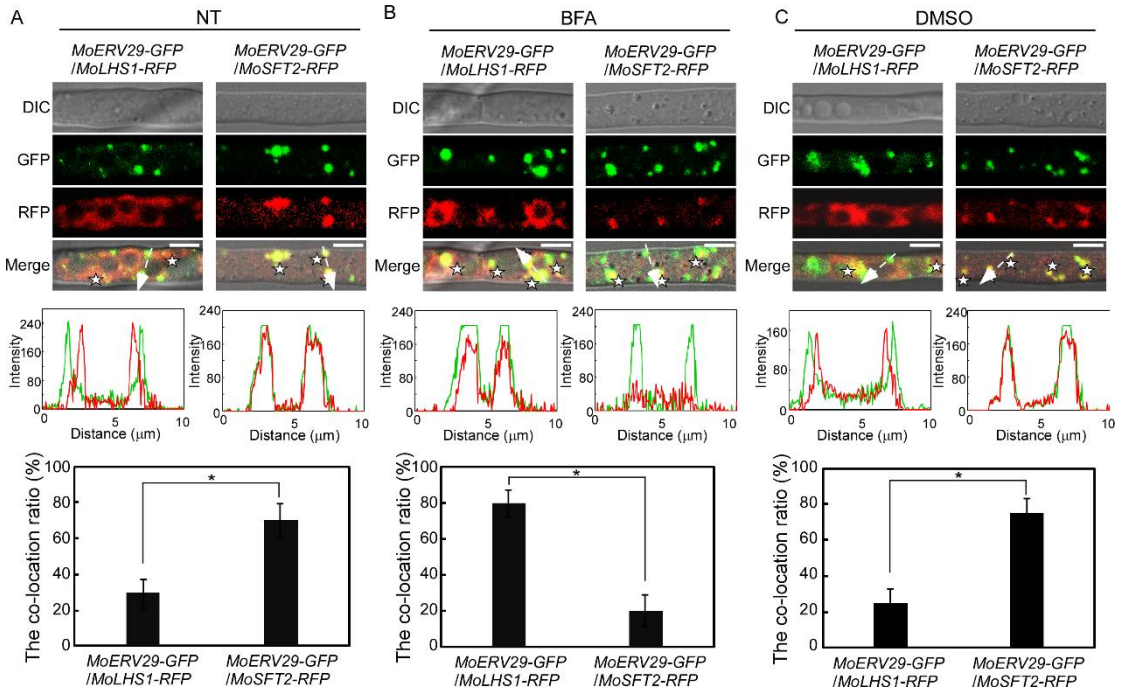

Figure S6. MoErv29 is dispensable for the secretion of cytoplasmic effectors AvrPiz-t and AvrPia.

BICs in the barley cells infected with strains expressing AvrPiz-t:GFP and Avr-Pia:GFP. Merged images show DIC and GFP channels. White asterisks indicate the BICs. In each experiment, 40 BICs were observed for each strain at 24 h post-inoculation (hpi). Bar = 10 μm.

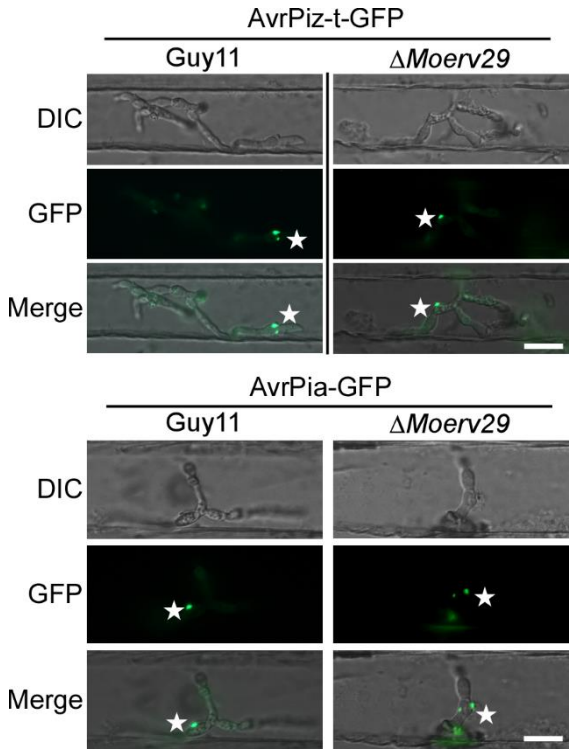

Figure S7. MoErv29 is not involved in the secretion of the apoplastic effector MoBas4.

MoBas4 was fused with GFP and transformed into Guy11 and Δ*Moerv29* mutant strains to observe the subcellular location. Bar = 10 μm.

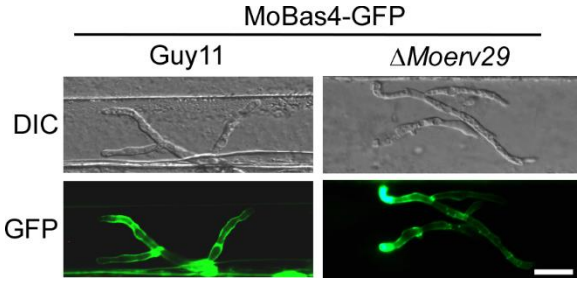

Figure S8. Identification of the putative cargo proteins regulated by MoErv29.

(A) Functional classification of identified MoErv29 cargo proteins based on Gene Ontology analysis. (B) KEGG pathway enrichment of the MoErv29 cargo proteins.

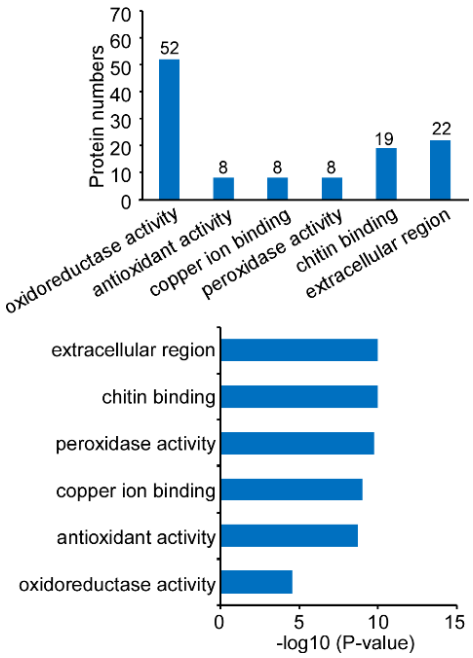

Figure S9. The Δ*Moerv29* mutants are impaired in the secretion of extracellular laccase and peroxidase.

(A and B) Guy11, Δ*Moerv29* mutant, and complemented strain were inoculated on CM medium containing 0.2 mM ABTS and 200 μg/ml Congo Red. The discoloration (ABTS) was monitored in complete media after three days of incubation, and discoloration of Congo Red was observed after incubation for five days. (C and D) The Guy11, Δ*Moerv29* mutants, and complemented strains were inoculated in CM liquid medium, and laccase activities were measured in the filtrate cultures using an ABTS oxidization test. The peroxidase activity was also measured by ABTS oxidization under H_2O_2 supplementation. Error bars represent the standard deviations, and asterisks represent significant differences ($p<0.01$).

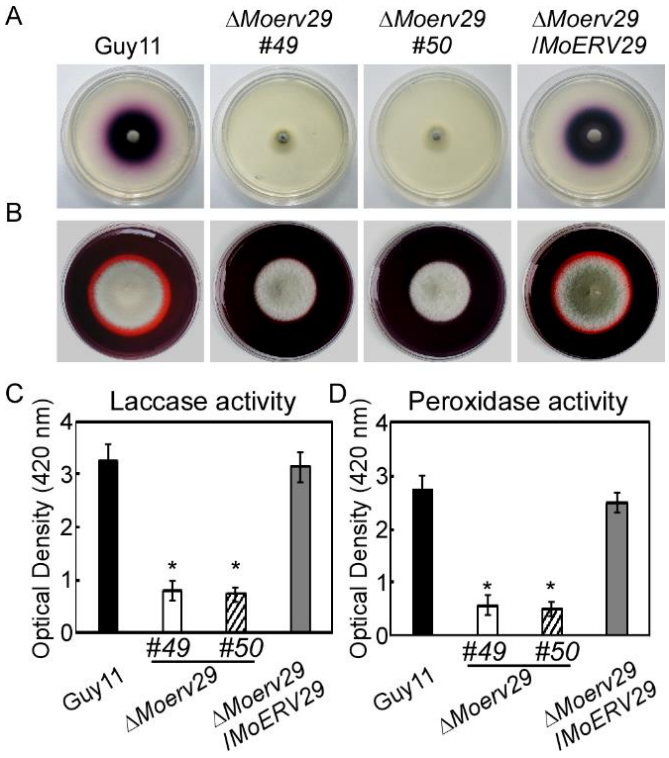

Figure S10. The gene expression pattern of putative effectors in MoErv29 cargo spectrum through qRT-PCR analysis.

Heat map showing expression levels of putative effectors in MoErv29 cargo spectrum during compatible interaction phases.

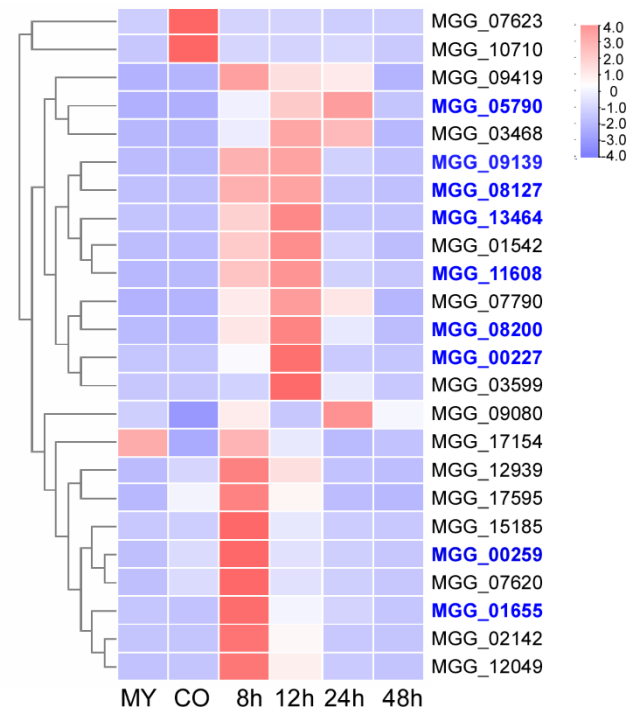

Figure S11. MoErv29 is not involved in the secretion of cytoplasm effector AvrPi9. AvrPi9 fused with GFP was transformed into Guy11 and the Δ*Moerv29* mutant strains to observe the subcellular location. Bar = 10 μm